

Mechanics of air-inflated 3D distance fabric

V. Votrubec^{a,*}, J. Žák^a

^aVÚTS, a. s., Svárovská 619, 460 01 Liberec, Czech Republic

Received 23 October 2020; accepted 12 May 2021

Abstract

3D distance fabrics are modern and promising material for lightweight inflatable structures. The applications are used in sport, boats, tents, construction, military etc. Its advantages are large load capacity per unit weight, stiffness dependent on pressurized air, fail-safe structure. However, the mechanics of inflated fabric panel is not still described enough. This paper gives basic theory and its experimental verification about mechanical behaviour of distance fabrics. The mathematical model of air-inflated distance fabric panel is created based on analytical theory of cylindrical bending of plates. Material data of the fabric required for performing computations of the model are determined from tensile tests. The reliability of the analytical model is experimentally verified. For that purpose the air-inflated fabric panel was made and tested. Results obtained both experimentally and analytically are compared and discussed. The experiment proves the validity of the mathematical model and allows us to predict the behaviour of distance fabrics.

© 2021 University of West Bohemia. All rights reserved.

Keywords: air-inflated distance fabrics, drop-stitch fabrics, 3D woven fabrics, mechanics of fabrics

1. Introduction

Distance fabrics also known as drop-stitch fabrics, double walled fabrics or spacer fabrics are a subset of 3D woven textiles. They consist of two (or more) skins – upper and lower fabric – which are simultaneously woven and connected by pile (drop) yarns (see Fig. 1). Pile yarns are the second type of warp yarns locking the skins together and creating very strong connection. Base fabrics are spaced apart by a distance given by the length of the pile yarns. This length is a parameter of a fabric and depends on weaving machine properties. It is usually constant so the inflated panel has parallel and uniform surfaces. It is also possible to weave distance fabrics with variable length of pile yarns. The skins are made impermeable by coating fabrics with an additional material (e.g., PVC, polychloroprene, etc.). The stability and load capacity of inflatable panels depend on their material properties, air pressure, fabric parameters and shape. During inflation, the air pressure causes biaxial pretensioning of fabric layers and elongation of pile yarns so the panel achieves the required shape and stiffness. The advantages of distance fabrics are lightweight structure and portability in non-inflated state. Its structure provides fail-safe mechanism during overload conditions where the fabric collapses without damage and regains its origin shape after removing the overload.

Today, most research effort is dedicated to 3D woven and knitted fabrics in general where yarns in the third axis are present and the thickness of fabric is not negligible. The survey of 3D woven fabrics can be found in [1, 4] or [6]. However, the field of distance fabrics has not been researched enough. The distance fabrics are suitable for filling the hollow with (compressed) air, sand or foam for sound insulation applications, sport equipment or army facilities. They are

*Corresponding author. Tel.: +420 485 302 387, e-mail: vlastimil.votrubec@vuts.cz.
<https://doi.org/10.24132/acm.2021.650>

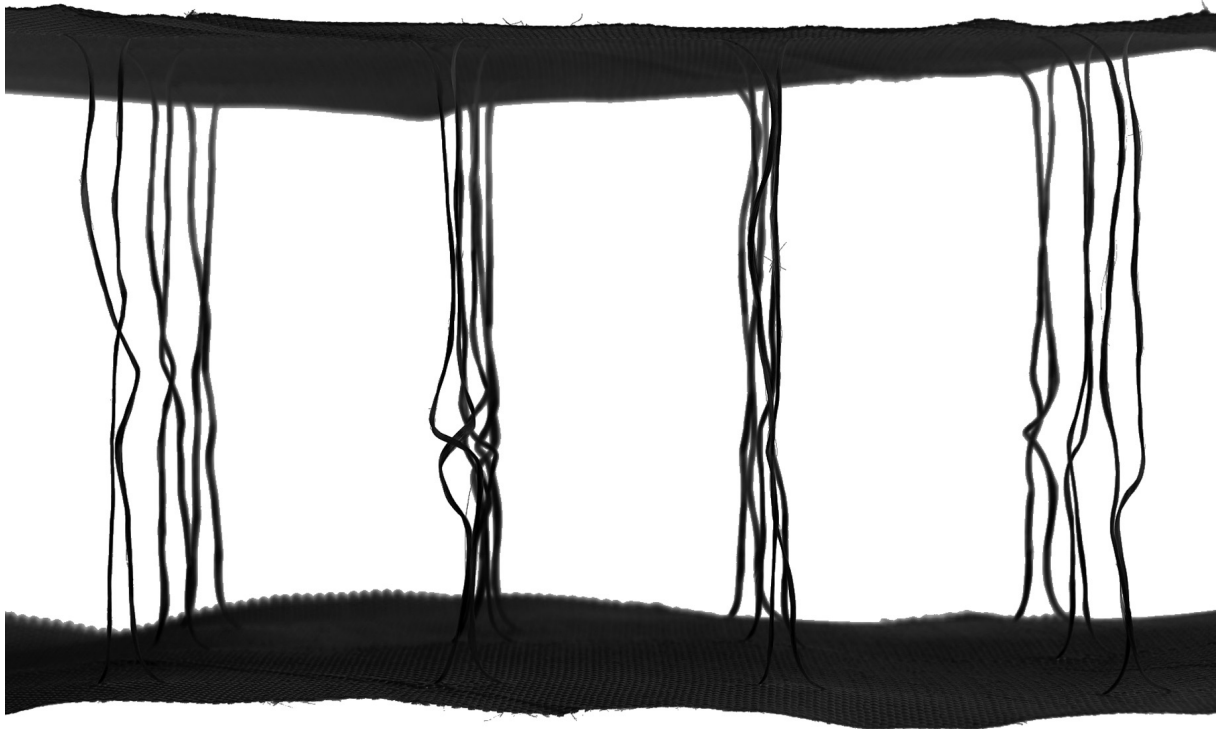


Fig. 1. Example of 3D fabric in non-loaded state

also suitable for working with gases, liquids or other materials as filters. Significant direction of development is focused on using these fabrics as reinforced composites [3]. This research is aimed at mechanics of air-inflated panels. Its intention is to describe forces acting in the fabric and shape of the fabric under the pressure of compressed air. Some research on inflatable fabric structures was performed earlier but only a few on distance fabric panels [5]. Cavallaro in [2] described the mechanics of a panel loaded by four point bending load. He used experimental data of material tests for his analytical model and performed also experiment of bended panel for comparison. Knitted spacer fabric was modelled by finite element method in [7].

The paper is structured as follows. Firstly, the mathematical model of the 2D fabric element is described. Then, the material testing methods and their results are shown and applied to the mathematical model. Finally, the experiment of inflating fabric panel is presented and results are compared and discussed. The conclusions and suggestions for further work are also given.

2. Theory

2.1. Equation governing skin deformation

Let us assume the linearity of the problem in the geometry and in the material behaviours together with the theory of thin plates, eliminating the influence of shear deformations. Then the mathematical theory of the 3D fabric skin mechanics can be based on the following differential equation describing cylindrical bending of thin plates:

$$\frac{d^2u}{dx^2} = \frac{M(x)}{E^*J}, \quad (1)$$

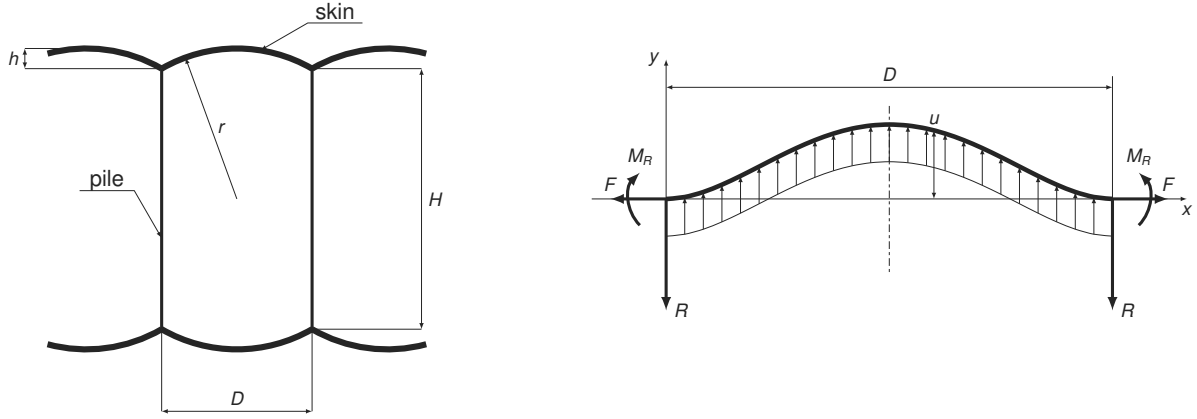


Fig. 2. Simplified schema of a loaded 3D fabric cell (left) and free body diagram of pressure loaded fabric skin (right)

where $E^* = \frac{E_x}{1-\nu_{xy}\nu_{yx}}$ with the assumption of plane strain in cylindrical bending and orthotropic material of skin (which may be – and actually is – orthotropic due to different warp and weft density) and $J = \int_{-\frac{t}{2}}^{\frac{t}{2}} y^2 dy$, t being the thickness of the skin; the material properties of the skin are supposed to be constant through the thickness.

Note that the bending stiffness $E^* J$ could be determined experimentally as a single value. The bending moment (see Fig. 2) as a function of x is

$$M(x) = M_R + F u + p \frac{(D-x)^2}{2} - R(D-x), \quad (2)$$

where p is internal air pressure; R and M_R are reaction force and moment, respectively, associated with pile force and plane of symmetry, and F is acting force in horizontal direction. All the quantities are related to unit length as commonly used in theory of plates. Actually, dimension of M in (1) or in (2) is $\frac{Nm}{m}$; there is also $[F] = [R] = \frac{N}{m}$ in the second relation. Substituting (2) into (1) we get the governing differential equation

$$\frac{d^2u}{dx^2} - \frac{F}{E^* J} u = \frac{1}{E^* J} \left(M_R + p \frac{(D-x)^2}{2} - R(D-x) \right). \quad (3)$$

2.2. Analytical solution and limit cases

The solution of governing equation may be written as follows:

$$u = \underbrace{C_1 e^{kx} + C_2 e^{-kx}}_{u_h} - \underbrace{\left(\frac{p}{2F} x^2 + \left(\frac{pD}{F} - \frac{R}{F} \right) x + \left(D \frac{R}{F} - \frac{M_R}{F} - \frac{pD^2}{2F} - E^* J \frac{p}{F^2} \right) \right)}_{u_p}, \quad (4)$$

where $k = \sqrt{\frac{F}{E^* J}}$.

The values of reaction force R , reaction moment M_R and integration constants C_1 and C_2 are given by boundary conditions

$$\begin{aligned} u(0) &= 0, \\ u(D) &= 0, \\ \left. \frac{du}{dx} \right|_{x=0} &= 0, \\ \left. \frac{du}{dx} \right|_{x=D} &= 0. \end{aligned}$$

Solution of the linear system gives the value $R = \frac{pD}{2}$, other relations are more complicated, e.g.:

$$C_1 = \frac{pD}{2F} \frac{1}{k} \frac{1}{e^{kD} - 1}.$$

Relation between C_1 a C_2 satisfies the condition of symmetry of the solution of homogeneous equation u_h around the middle point $x = \frac{D}{2}$:

$$C_2 = C_1 e^{kD} \longrightarrow u_h = C_1 (e^{kx} + e^{k(D-x)}).$$

Thus, the relation (4) becomes

$$u = C_1 (e^{kx} + e^{k(D-x)}) - \frac{p}{2F} x^2 + \left(\frac{pD}{F} - \frac{R}{F} \right) x + D \frac{R}{F} - \frac{pD^2}{2F} - \frac{M_R}{F} - E^* J \frac{p}{F^2}.$$

Reordering individual terms we get the previous equation in the following form:

$$u = C_1 (e^{kx} + e^{k(D-x)}) - \frac{p}{2F} (D-x)^2 + \frac{R}{F} (D-x) - \frac{M_R}{F} - E^* J \frac{p}{F^2}. \quad (5)$$

Evaluating the solution for the case $F = 0$, we get the limit case of (4) or (5):

$$\lim_{F \rightarrow 0} u(x) = \frac{p}{24 E^* J} x^2 (D-x)^2,$$

which corresponds to the common solution of two-side clamped plate.

Another limit case for $E^* J = 0$, i.e., a plate with vanishing bending stiffness, gives:

$$\lim_{E^* J \rightarrow 0} u(x) = \frac{p}{2F} x (D-x).$$

Obviously by using the relation $\frac{d^2 u}{dx^2} \doteq \kappa = \frac{1}{r}$ we obtain a constant curvature $\kappa = -\frac{p}{F}$, or $r = -\frac{F}{p}$, so that the deformed shape is closing a circular arc, which again corresponds to the idea of a pressure loaded perfectly flexible cylindrical membrane.

Both above mentioned limit cases demonstrate that used theory can be seen as an integration of the theory of cylindrical bending of thin plates and the theory of pressure loaded cylindrical membranes.

2.3. Acting forces

It is the value of F , which is assumed to be constant along x , that has the main influence on the final shape of deformed fabric skin. If we suppose both ends of the plate to be clamped and D to be constant, then the force F can be obtained from the equation of elongation of the central line. If the value D varies, the force F can be obtained from equilibrium equation in x direction

$$F \doteq \frac{pH}{2}, \quad (6)$$

where H is the height of 3D distance fabric, under the assumption that $u_{\max} \ll H$ is fulfilled. Finally, it is this approach we have opted for. Substituting (6) into (5) we get

$$u = \frac{D}{H} \frac{1}{k} \frac{e^{k(D-x)} + e^{kx}}{e^{kD} - 1} - \frac{(D-x)^2}{H} + \frac{D}{H} (D-x) - \frac{2M_R}{pH} - \frac{4E^*J}{pH^2}. \quad (7)$$

Using the relation (6), the parameter k becomes here $k = \sqrt{\frac{pH}{2E^*J}}$.

If $x = D$ in (7), we can obtain the value M_R by using boundary condition $u(D) = 0$:

$$2M_R = \frac{pD}{k} \frac{e^{kD} + 1}{e^{kD} - 1} - \frac{4E^*J}{H}.$$

2.4. Resulting relation

The final relation for u then becomes

$$u = \frac{D}{H} \frac{1}{k} \left(\frac{e^{k(D-x)} + e^{kx}}{e^{kD} - 1} - \frac{e^{kD} + 1}{e^{kD} - 1} \right) - \frac{(D-x)^2}{H} + \frac{D}{H} (D-x). \quad (8)$$

In equation (8), the last two on loading independent terms represent a parabolic function which replaces the circular arc in case of small displacements, i.e., the shape function of an ideal pressure loaded cylindrical membrane. The first term then represents a deviation due to non zero bending stiffness of a plate-like fabric skin.

Another parameter of interest is the *arc* height h (see Fig. 2). It is defined by the value of u at $x = \frac{D}{2}$:

$$h = \frac{D}{Hk} \frac{2e^{\frac{kD}{2}} - e^{kD} - 1}{e^{kD} - 1} + \frac{D^2}{4H}.$$

Note that according to Fig. 2, the exact solution of radius of a bending free membrane-like fabric skin of this 3D distance fabric is given by

$$r = \frac{\sqrt{D^2 + H^2}}{2}, \quad \text{thus,} \quad u\left(\frac{D}{2}\right) = h = \frac{\sqrt{D^2 + H^2} - H}{2}.$$

2.5. Graphic representation of theoretical results

Besides the maximal value of deflection itself we have opted for an evaluation of curvature radius of the deformed shape to better appreciate the differences between the deformation of a membrane-like skin and a skin with non zero bending stiffness. Let this radius be defined in accordance with (1) by

$$r \doteq \frac{1}{u''}, \quad (9)$$

where u is given by (8). The resulting graphics of the theoretical values of u and r are presented in Fig. 3.

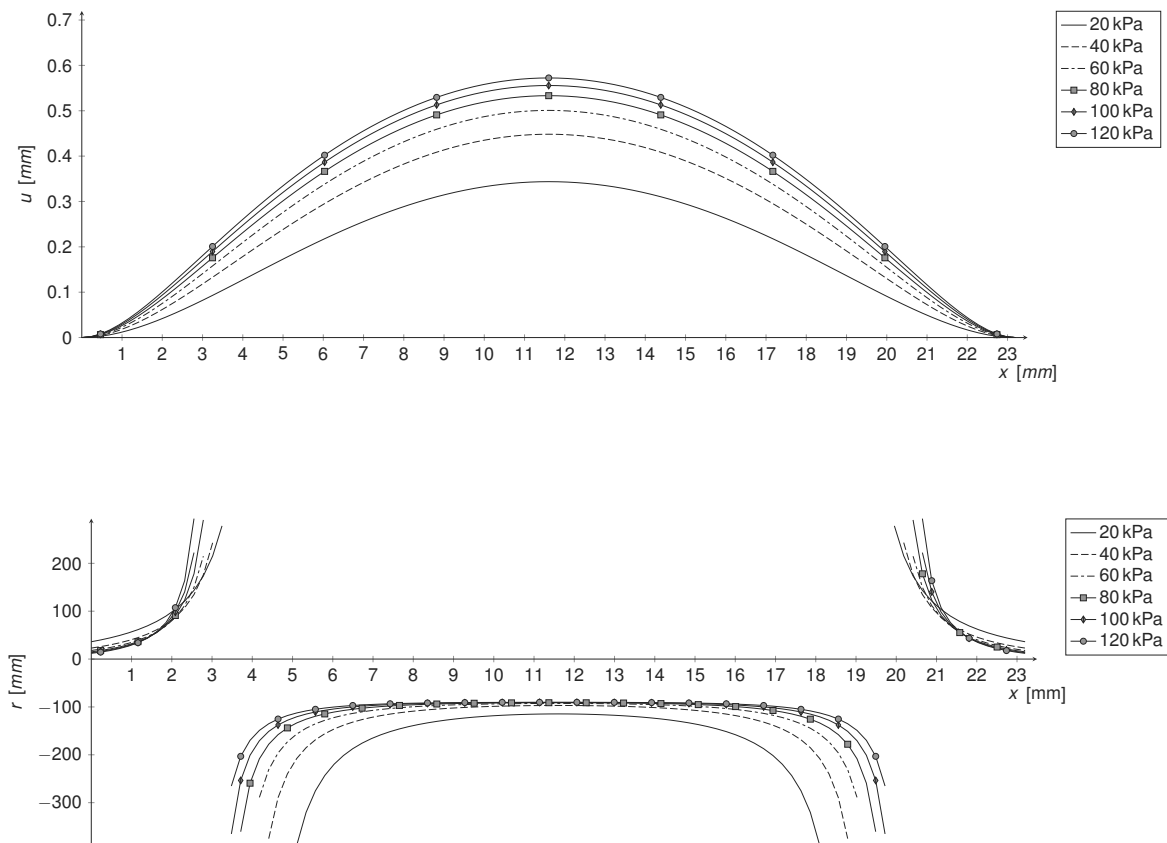


Fig. 3. Graphics of theoretic deflection (top) and associated curvature radius (bottom)

3. Experiment

3.1. Description of experiment arrangement

The panel used for testing (see Fig. 4) was made from the fabric roll. This roll is composed of polyester (PES) fabric woven on DIFA weaving machine developed and produced by VÚTS, a.s. The outer sides of 3D-fabric skins were then coated by polychloroprene (Neoprene) impregnated fabric in order to make the 3D-fabric airtight. The size of fabric sample was approximately 100×100 cm. Its edges were glued together and clamped by several screwed steel flat bars. These bars allow the panel to deform freely and hold the air inside. There were two pipes leading into the panel. One pipe is used for air inflating of the panel and the second one for measurement of static pressure inside the panel.

The profile of the fabric skin was measured by a compact laser scanner Micro-Epsilon scanControl 2950-100/BL (see Fig. 5). It recorded 1280 points on 100 mm long line segment across the cells, so at least two whole profile cells of the fabric were scanned (see Fig. 6).

The panel was gradually inflated and static pressure and profile of the fabric were recorded for each step of 10 kPa in the range from 40 kPa to 120 kPa. The testing was terminated at the pressure level of 120 kPa due to safety of the measurement device. This measuring range of static pressure is sufficient because the operating pressure in common sport applications (paddle boards, boats) is around 100 kPa.



Fig. 4. Panel used in tests in fully inflated condition



Fig. 5. Arrangement of measuring device

3.2. Measured data analysis

Recorded sets of coordinates were statistically processed using symbolic mathematical software Maxima. The linear trend of the measured data due to a slight non-perpendicularity of measurement device was removed using linear regression and data were shifted to the null position with the horizontal axis located at the resulting mean value A_0 . Variation of A_0 can also be understood as the elongation of pile yarns. Measured data are partly presented in the upper graph of Fig. 6. The increase of constant term A_0 of resulting linear regression as a function of applied pressure is depicted in Fig. 8.

As mentioned in Section 2.5, the radius of curvature is used to evaluate the deformed shape of the skin. Using this definition the radius is determined as follows:

1. The curvature radius r is defined by the relation (9).
2. The function u used in (9) is replaced by a function \bar{u} based on the measured data.
3. This function \bar{u} can be determined by using linear regression on a set of measured points, e.g., points distributed over an arbitrary interval of measured field; this regression function \bar{u} should be in such form to cover eventual inflection points, e.g., a polynomial P of sufficiently high degree N :

$$\begin{bmatrix} P_0 \\ P_1 \\ \vdots \\ P_N \end{bmatrix} = \begin{bmatrix} \sum_{m=s-d}^{s+d} 1 & \sum_{m=s-d}^{s+d} x_m & \cdots & \sum_{m=s-d}^{s+d} x_m^N \\ & \sum_{m=s-d}^{s+d} x_m^2 & & \sum_{m=s-d}^{s+d} x_m^{N+1} \\ & & \ddots & \vdots \\ & & & \sum_{m=s-d}^{s+d} x_m^{2N} \end{bmatrix}^{-1} \times \begin{bmatrix} \sum_{m=s-d}^{s+d} y_m \\ \sum_{m=s-d}^{s+d} (x_m y_m) \\ \vdots \\ \sum_{m=s-d}^{s+d} (x_m^N y_m) \end{bmatrix}$$

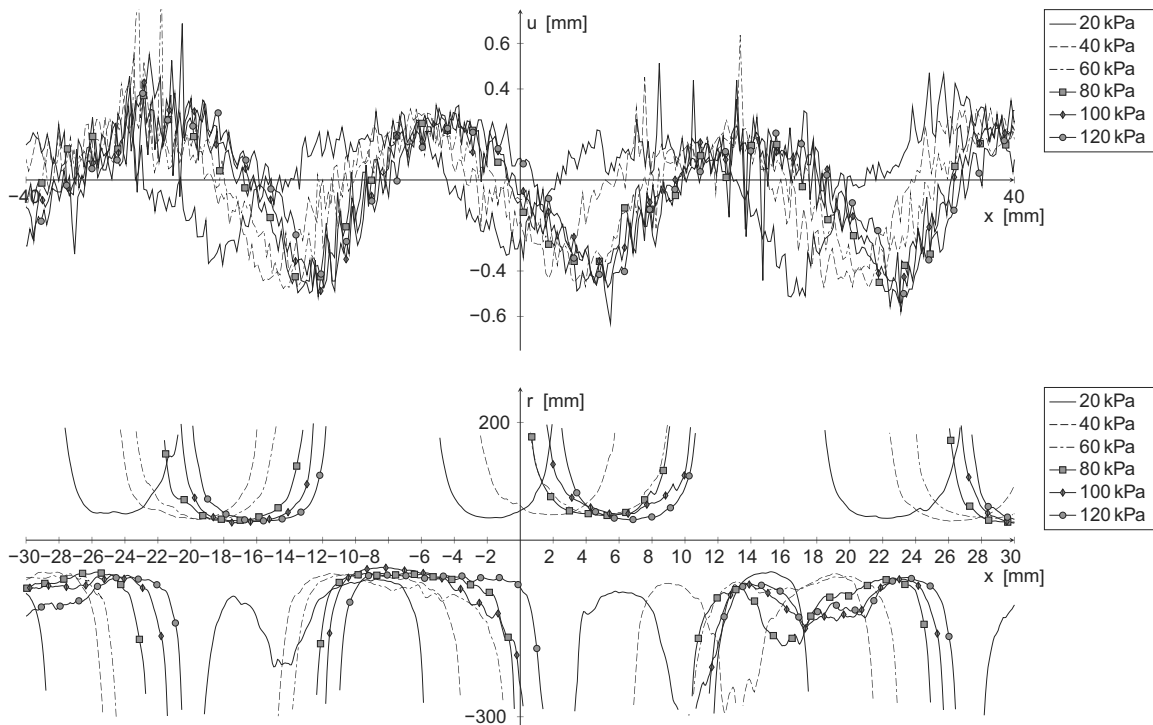


Fig. 6. Measured deflections (top) and calculated curvature radius (bottom)

4. The value of $\bar{r} = \frac{1}{\bar{u}'}$ is then evaluated at the midpoint s at the position x_s of interval $\langle x_{s-d}, \dots, x_s, \dots, x_{s+d} \rangle$:

$$\bar{r}_s = \bar{r}(x_s) \doteq \frac{1}{\sum_{i=2}^N i(i-1) P_k x_s^{i-2}}.$$

5. The values of \bar{r}_s are evaluated at all points of measured domain, with exception of d points near the ends, where sufficient data are not available.

In the presented work, we have used a polynomial function of degree $N = 4$ and a sampling interval of $2d = 270$ points which represents approximately 21 mm long section of the measured field. For the actual pitch D of the binding yarns of about 23.2 mm (see Fig. 2), the sampling interval covers almost 90% of its length. The values of curvature determined by this way are presented in the bottom part of Fig. 6.

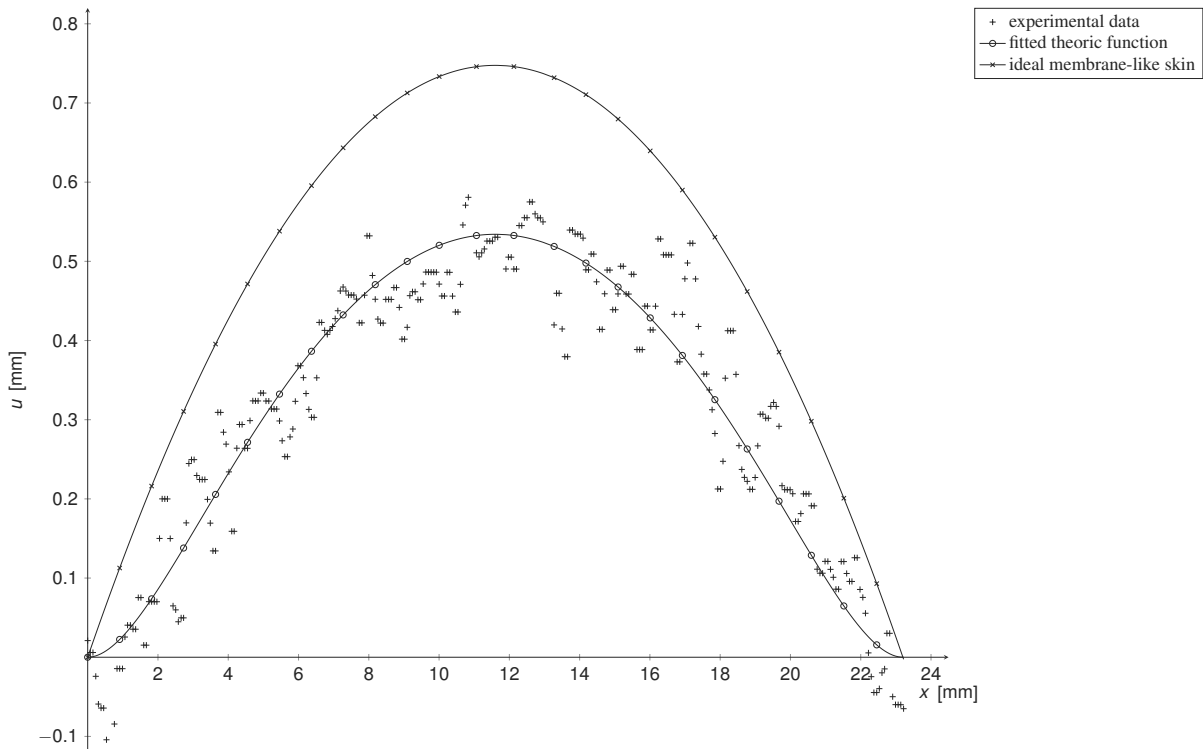


Fig. 7. Experimental data for $p = 100$ kPa fitted with a function in the form of relation (8)

The function fit was carried out on an arbitrary chosen interval of measured data using least squares method in Mathematica software, see Fig. 7. Used fitting function was in the form of (8) resulting from the theoretic analysis of the problem.

3.3. Discussion of results

A relative shift of skins (a shear of 3D fabric) due to non-perpendicularity of binding yarns during the inflation, complicates the evaluation of the measured data. The main cause of the evaluation difficulty can be seen in the processing of the data mentioned in Section 3.2. While

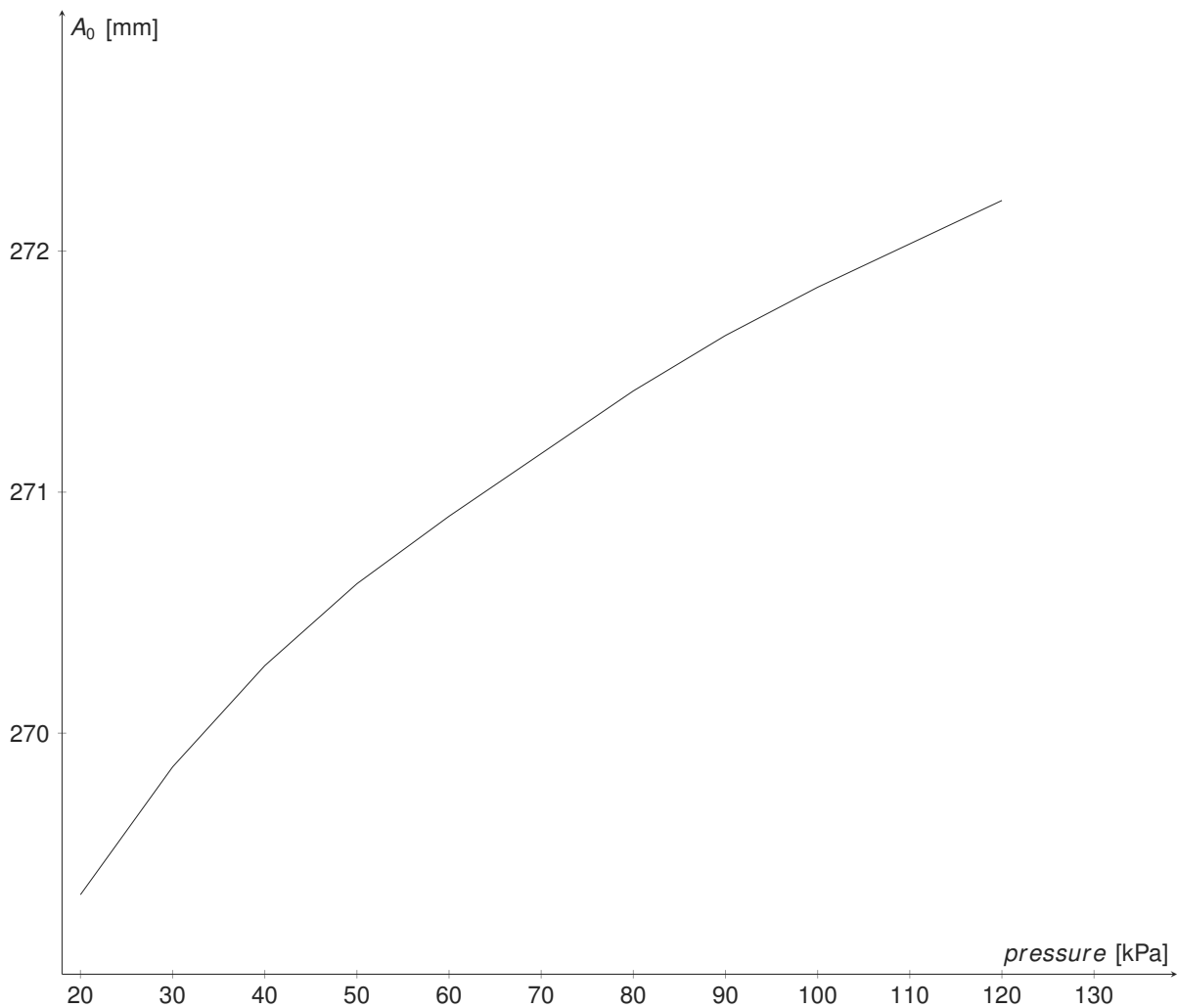


Fig. 8. Linear regression mean value as defined in 3.2

the constant terms in the resulting linear regression are in agreement with the expected behaviour of inflating fabric panel (see Fig. 8), the linear term is significantly influenced by the translation and simple subtraction of the linear trend, which may indicate that the chosen approach may not be necessarily correct. Because the processed data show a certain linear trend, it is only natural that they influence the consequent processing.

The measurement using laser scanner is very precise, even to such a degree that filtration of individual binding points of the fabric could be possible. This accuracy of measurement causes a difficulty, because the measured profile is not completely parallel to warp fibres. It means that the scanning laser beam crosses the warp fibre while the optimal trajectory leads along that fibre. With respect to the magnitude of the measured deflection in the range of 0.5 mm, the fibre height of approximately 0.1 mm is not negligible.

Potential source of measurement inaccuracy and relatively distinct noise could be the experiment realization that was due to safety reasons executed outside (see Fig. 5) and therefore it was influenced by meteorological effects, such as variable wind and solar radiation. Potential dirt on fabric surface could also influence the surface reflection depending on exposure (see the extreme values of deflections in Fig. 6). However, measurements were performed repeatedly and the trend was confirmed.

4. Conclusions

The mathematical theory of mechanical behaviour of air-inflated 3D distance fabrics was presented. It is based on combination of the theory of thin plates and membrane theory. From the basic relations of mentioned theories and specific limitations of this case, the final equation (8) describing the deflection u of the skin is derived. Although the simple approach is used, the results are valuable and correspond to the measured data.

The reason for the noted discrepancies between theory and experiment may be found in the non-linear behaviour of composite materials and the varying stiffness $E^* J$ of the fabric skin, which is dependent on the bending orientation. It is caused by different composition of outer skin layers. The lower (inner) layer of fabric skin – PES fabric has very low (practically zero) stiffness in compression (dry non-saturated fabric), so it contributes to bending stiffness only if it is on the tensile side (near the pile – skin joint). Then the bending stiffness is higher than if the PES fabric is compressed. Moreover the situation is complicated by the pre-tensioning of the fabric, which does not allow to calculate stress in the outer layer based only on curvature $\kappa \doteq \frac{d^2u}{dx^2}$. This fact leads to a solution of non-linear problem that is defined on two separate sections of examined interval D . These intervals are of different length of unknown value, where the tension and the bending properties of a fabric skin differ. However, the solution of the non-linear problem could not be easily found by mathematical analysis methods and now it is a subject of computations using the finite element method. The numerical solution then allows to take into account also the geometrical nonlinearity that is neglected in the presented work.

Even when all mentioned limitations are considered, we are able to evaluate the deflections and combined stresses of the 3D fabric skin. The presented theory is proved by experimentally obtained data and it allows us to predict mechanical behaviour of 3D distance fabrics.

Acknowledgements

This publication was supported by the Czech Ministry of Industry and Trade in the framework of the institutional support for long-term conceptual development of research organization – recipient VÚTS, a. s.

References

- [1] Badawi, S. S., Development of weaving machine and 3D woven spacer fabric structures for lightweight composites materials, Ph.D. Thesis, Technical University in Dresden, Dresden, Germany, 2007.
- [2] Cavallaro, P. V., Hart, C. J., Sadegh, A. M., Mechanics of air-inflated drop-stitch fabric panels subject to bending loads, Proceedings of ASME International Mechanical Engineering Congress and Exposition, ASME, 2013, IMECE2013-63839. <https://doi.org/10.1115/IMECE2013-63839>
- [3] Chen, X., Taylor, L. W., Tsai, L. J., An overview on fabrication of three-dimensional woven textile preforms for composites, *Textile Research Journal* 81 (2011) 932–944. <https://doi.org/10.1177/0040517510392471>
- [4] Chen, X., *Advances in 3D Textiles*, Woodhead Publishing, 2015.
- [5] Falls, J., Waters, J. K., Bending test of inflatable dropstitch panel, Proceedings of the 11th International Conference on Fast Sea Transportation, Hawaii, USA, 2011.

- [6] Gokarneshan, N., Alagirusamy, R., Weaving of 3D fabrics: A critical appreciation of the developments, *Textile Progress* 41 (1) (2009) 1–58. <https://doi.org/10.1080/00405160902804239>
- [7] Hou, X., Hu, H., Silberschmidt, V. V., A study of computational mechanics of 3D spacer fabric: Factors affecting its compression deformation, *Journal of Materials Science* 47 (2012) 3989—3999. <https://doi.org/10.1007/s10853-012-6252-2>